Received: Added at production | Revised: Added at production | Accepted: Added at production

DOI: xxx/xxxx

RESEARCH ARTICLE

Heading control based on extended homogeneous polynomial Lyapunov function

Yanwei Huang* | Feng Lin

College of Electrical Engineering and Automation, Fuzhou University, Fuzhou, China

Correspondence
Yanwei Huang, College of Electrical Engineering and Automation, Fuzhou University, Fuzhou 350116, China.
Email: sjtu_huanghao@fzu.edu.cn

Funding Information
This research was supported by the Science and Technology Guidance Project of Fujian (2019H0007) and the National Natural Science Foundation of China (51977040)

Summary

For the nonlinear parameter-varying (NPV) model of unmanned surface vehicle (USV) with the consideration of the velocities on yaw and surge as well as wave disturbances, a robust H_∞ control method is proposed based on extended homogeneous polynomial Lyapunov function (EHPLF) to regulate heading for the superior performance on the rapidity, accuracy and robustness. Firstly, a NPV model of heading error is established to design a general form of a state feedback controller with a robust H_∞ performance. Secondly, a Lyapunov matrix with full states and varying parameter is constructed to derive the robust H_∞ global exponential stability conditions by Euler's homogeneity relation for the NPV system, known as the EHPLF stability conditions. Thirdly, since the EHPLF stability conditions consist of a set of nonlinear coupled inequalities that cannot be directly solved by sum of squares (SOS) toolboxes, they are decoupled with matrix transformations to obtain the EHPLF-SOS stability conditions, which is solved for the parameters of the state feedback controller. Finally, the simulation results indicate that EHPLF method exhibits a superior performance on dynamic, steady-state and robustness.

KEYWORDS:
heading control, nonlinear parameter-varying (NPV) model, robust H_∞ control, extended homogeneous polynomial Lyapunov function (EHPLF), sum of squares (SOS)

1 | INTRODUCTION

Unmanned Surface Vehicle (USV) has complex dynamics and is susceptible to parameter uncertainties and external disturbances such as waves, currents, and so on. These prominent nonlinear and time-varying characteristics deteriorate the performance of heading control for USV. [1,2] Therefore, it is of great significance to study a heading control method for an advanced model of USV to improve the rapidity and accuracy of heading regulation and ensure the system robustness. [3,4]

Heading control technology has always been a research hotspot in USV academic fields. A μ-Synthesis robust controller is designed to suppress the uncertainties of Nomoto model and the disturbances caused by waves. [5] To solve the mass-varying problem of USV during navigation, a heading linear parameter-varying (LPV) model with mass-varying parameters is controlled by a dynamic output feedback H_∞ method based on improved bounded real lemma. [6] Considering the influence of varying surge velocity on heading control, a LPV model with surge velocity is established and controlled by a state feedback H_∞ heading control method to suppress the adverse effects of surge velocity changes and external disturbances on heading regulation. [7] However, it is difficult for LPV model to accurately describe the hydrodynamic nonlinear characteristics of USV. For the nonlinear Norrbin model with uncertain parameters, a robust H_∞ heading control method based on convex hull is proposed to effectively suppress the adverse effect of system uncertainty.[8] For the Fossen model with asymmetric inertia matrix and damping coefficient matrix, a nonlinear heading error model is established to propose a static output feedback H_∞ heading control method based on extended bounded real lemma.[9] Nonlinear parameter-varying (NPV) systems retain the advantages of both nonlinear and varying parameter, including the nonlinear problem of yaw motion and varying parameter of surge velocity[10,11,12]. The nonlinear matrix inequality (NLMI) solution conditions are derived for NPV H_∞ heading controller by constructing a parameter-dependent quadratic Lyapunov function (QLF).[13] However, the parameter-dependent QLF matrix is only introduced with varying parameter and without state variables, which to some extent restricts the performance on dynamic, steady-state and robustness.[14] Therefore, it is challenging to explore a Lyapunov matrix with full states and varying parameter to design a robust H_∞ control method for NPV system.

Compared to QLF, a polynomial Lyapunov function (PLF) is used to control nonlinear system to improve system performance by the solution of the non-convex problem for the stability conditions.[15,16,17] Non-convexity can be avoided by assuming that the PLF matrix depends only on the state variables corresponding to the zero rows in the input matrix.[18] The robust stability conditions for a NPV system are derived by constructing a PLF matrix which introduces a varying parameter and partial state variables.[10] However, this method is limited to a class of systems with the zero rows in input matrix, and the degree of dependence of state variables depends on the number of the zero rows in the input matrix, which generally means that Lyapunov matrix cannot be introduced with full state variables. To some extent, this limits the freedom degree of the construction of parameter-dependent Lyapunov function for the controller design which will affect the system performance. A homogeneous polynomial Lyapunov function (HPLF) is introduced to improve the performance of nonlinear system.[19,20,21] HPLF not only overcomes by the Euler's homogeneity relation the non-convex problem which caused by the derivation of the high-order PLF matrix, but also solves the problem that PLF is limited by the zero rows of input matrix. However, HPLF matrix does not consider the problem of varying parameter. Therefore, it is a key technology for HPLF to be constructed with full states and varying parameter in designing robust controllers for NPV system.

Aiming at NPV model with the nonlinear varying characteristics, a robust H_∞ heading control method based on extended HPLF (EHPLF) is proposed to improve the rapidity, the accuracy and the robustness of heading regulation. Firstly, a NPV model of heading error is established with yawing and varying surge velocity. Under the conditions of robust H_∞ stability, a general controller form of NPV closed-loop system is designed by the principle of state feedback control. Secondly, a Lyapunov matrix with full state variables and varying parameter is constructed to obtain the robust H_∞ EHPLF exponential stability conditions. Thirdly, the EHPLF stability conditions with nonlinear coupling terms cannot be directly solved by sum of squares (SOS) toolboxes. The matrix transformation is used to decouple the EHPLF stability conditions for the EHPLF-SOS stability conditions, which can be directly solved by SOS toolboxes for the controller parameters. Finally, the simulation results indicate that the proposed control method exhibits superior dynamic, steady-state and robustness performance through the comparison.

The matter of this paper is organized as follows. In Section 2, a NPV model of heading error is given. In Section 3, the robust H_∞ global exponential stability conditions known as EHPLF stability conditions are presented to transform into EHPLF-SOS stability conditions to design NPV heading controller. The numerical simulations are presented in Section 4, exhibiting a superior advantages of EHPLF method. Concluding remarks are made in Section 5.

2 | NPV MODEL OF HEADING ERROR

In the horizontal plane, USV is assumed as a three-degree-of-freedom motion of surge, sway and yaw. USV dynamics model is[22]

$$M\dot{\nu} + C(\nu)\nu + D(\nu)\nu = \tau + \tau_w, \tag{1}$$

where $\nu = \begin{bmatrix} u & v & r \end{bmatrix}^T$ is the velocity vector, u,v and r are surge, sway and yaw velocity, $\begin{bmatrix} u & v & r \end{bmatrix}^T$ is the transpose matrix of $\begin{bmatrix} u & v & r \end{bmatrix}$, $\tau = \begin{bmatrix} \tau_u & 0 & \tau_r \end{bmatrix}^T$ is the vector of the longitudinal thrust τ_u and the yaw moment τ_r, $\tau_w = \begin{bmatrix} \tau_{uw} & \tau_{vw} & \tau_{rw} \end{bmatrix}^T$ is the disturbance vector, τ_{uw}, τ_{vw}, and τ_{rw} represent the external disturbances of the surge, sway and yaw motion respectively. M is the inertia matrix. $C(\nu)$ is the Coriolis and centripetal matrix. $D(\nu)$ is the damping coefficient matrix.

(1) can be transformed into a general form of the state-space representation for the nonlinear system as

$$\dot{\nu} = A(\nu)\nu + B_1\tau_w + B_2\tau, \tag{2}$$

where $A(\nu) = -M^{-1}(C(\nu) + D(\nu))$, M^{-1} is the inverse matrix of M, $B_1 = B_2 = M^{-1}$.

Since the sway velocity υ is assumed as very small, i.e., $\upsilon \approx 0$, the sway motion model and the coupling terms with υ can be neglected. Moreover, the surge velocity u is assumed as a varying parameter $\sigma(t)$. For (2), NPV model of heading error can be derived as [13]

$$\begin{aligned} \dot{x} &= A(x, \sigma(t))x + B_1 w + B_2 u_\tau, \\ z &= Cx + D_1 w + D_2 u_\tau, \end{aligned} \tag{3}$$

where $x = \begin{bmatrix} r & \psi_e \end{bmatrix}^T$, the heading angle error $\psi_e = \psi_d - \psi$, ψ_d is the desired heading angle, ψ is the measured heading angle, controller output $u_\tau = \begin{bmatrix} \tau_r & 0 \end{bmatrix}^T$, external disturbance $w = \begin{bmatrix} \tau_{rw} & 0 \end{bmatrix}^T$. $A(x, \sigma(t)) = \begin{bmatrix} c_1\sigma(t) + c_2\sigma^2(t) + c_3 r^2 & 0 \\ -1 & 0 \end{bmatrix}$, $B_1 = B_2 = \begin{bmatrix} c_4 & 0 \end{bmatrix}^T$, $C = \begin{bmatrix} 0 & 1 \end{bmatrix}$, $D_1 = D_2 = \begin{bmatrix} 0 & 0 \end{bmatrix}^T$, $c_i (i = 1, 2, 3, 4)$ are the NPV model parameters.

3 | NPV HEADING CONTROLLER BY EHPLF

3.1 | State feedback controller with robust H_∞ performance

For NPV model (3), the state feedback controller is designed as

$$u_\tau = K(x, \sigma(t))x. \tag{4}$$

With (3) and (4), the closed-loop system of NPV is

$$\begin{aligned} \dot{x} &= \hat{A}(x, \sigma(t))x + B_1 w, \\ z &= \hat{C}x + D_1 w, \end{aligned} \tag{5}$$

where

$$\begin{aligned} \hat{A}(x, \sigma(t)) &= A(x, \sigma(t)) + B_2 K(x, \sigma(t)), \\ \hat{C} &= C + D_2 K(x, \sigma(t)). \end{aligned} \tag{6}$$

For (5), it is useful for robust H_∞ control technology to suppress system parameter uncertainties and external disturbances. For any initial system state $x(t_0)$, if the system state and the integral inequality J with the control output z and the disturbance w satisfy the inequalities: [9,23]

$$\|x(t)\| < be^{-\kappa(t-t_0)} \left\|x(t_0)\right\|, \forall t \geq t_0 \geq 0, \tag{7}$$

$$J = \int_0^\infty (z^T z - \gamma^2 w^T w)dt < 0, w \in L_2(0, \infty], \tag{8}$$

where $\|\cdot\|$ denotes a suitable norm (e.g., Euclidean norm), $b > 0$ and $\kappa > 0$ are constants, $\gamma > 0$ is the H_∞ performance criteria. (7) and (8) mean that the system is globally exponentially stable with the robust H_∞ performance. Moreover, for any initial state of the system, the system state decays exponentially and stabilizes within a bounded range as time t approaches infinity. These implies that the system possesses global exponential stability and eventually converge to a bounded stable state, regardless of the initial state.

3.2 | EHPLF stability conditions

To achieve global exponential stability and H_∞ performance for the closed-loop system (5), it is necessary to design an NPV controller (4) with the conditions of (7) and (8). Since both the method of PLF and the method of QLF restrict the system performance [10,13], EHPLF matrix with full states and varying parameter for NPV system is proposed to improve system performance.

For the closed-loop system(5), EHPLF is designed as

$$V(x, \sigma(t)) = x^T P(x, \sigma(t))x, \tag{9}$$

where $P(x, \sigma(t))$ is EHPLF matrix with full states and varying parameter.

The general form of EHPLF (9) is rewritten as

$$V(\xi) = \xi^T T(\xi)\xi, \tag{10}$$

where $\xi = \begin{bmatrix} x \\ \sigma(t) \end{bmatrix}$, $T(\xi) = \begin{bmatrix} T_{11}(x,\sigma(t)) & T_{12}(x,\sigma(t)) \\ T_{12}^T(x,\sigma(t)) & T_{22}(x,\sigma(t)) \end{bmatrix} = \begin{bmatrix} P(x,\sigma(t)) & 0 \\ 0 & 0 \end{bmatrix}$ is a homogeneous polynomial symmetric matrix, the 0 represents the zero matrix of appropriate dimensions. Compared to HPLF, EHPLF considers not only the full state x, but also the varying parameter $\sigma(t)$, specially for NPV system.

Lemma 1 (Euler's homogeneity relation [19])**.** If $V(x)$ is a homogeneous polynomial function of degree g, the following relation holds

$$gV(x) = x^T \nabla_x V(x) = \nabla_x V(x)^T x, \tag{11}$$

where $\nabla_x V(x) = \partial V(x)/\partial x$ is the gradient of $V(x)$ with respect to x.

Theorem 1. NPV closed-loop system (5) is globally exponentially stable with a robust H_∞ performance by the form of the state feedback controller (4) under the EHPLF stability conditions as

$$\eta_1^T (P(x,\sigma(t)) - \varepsilon_1 I)\eta_1 \geq 0, \tag{12}$$

$$\eta_2^T (\varepsilon_2 I - P(x,\sigma(t)))\eta_2 \geq 0, \tag{13}$$

$$\eta_3^T \left(\Pi + \varepsilon_3 I\right) \eta_3 \leq 0, \tag{14}$$

where

$$\Pi = \begin{bmatrix} \Theta & \frac{g}{2} P(x,\sigma(t))B_1 & \hat{C}^T \\ * & -\gamma^2 I & {D_1}^T \\ * & * & -I \end{bmatrix}, \tag{15}$$

$$\Theta = \frac{g}{2} he(X) + \alpha P(x,\sigma(t)), \tag{16}$$

$$X = \hat{A}^T(x,\sigma(t))P(x,\sigma(t)), \tag{17}$$

$he(X) = X + X^T$, $P(x,\sigma(t))$ is a positive definite symmetric EHPLF matrix, $K(x,\sigma(t))$ is a polynomial state feedback gain matrix, $\varepsilon_i > 0 (i = 1,2,3)$ are constants and $\varepsilon_2 > \varepsilon_1$, $\alpha > 0$ is the exponential decay coefficient, $*$ is a symmetric block of the symmetric matrix, $\eta_i (i = 1,2,3)$ are column vectors of proper dimensions, the I is the identity matrix of appropriate dimensions.

Proof. from (12) and (13), the relation is

$$0 < \varepsilon_1 x^T x \leq x^T P(x,\sigma(t))x \leq \varepsilon_2 x^T x. \tag{18}$$

With (10), (18) is

$$0 < \varepsilon_1 \|x\|^2 \leq V(\xi) \leq \varepsilon_2 \|x\|^2. \tag{19}$$

$V(\xi)$ is positive definite and bounded from (19).

Since Lemma 1 of a homogeneous polynomial function $V(\xi)$, the gradient of $V(\xi)$ with respect to ξ is

$$\nabla_\xi V(\xi) = \frac{1}{g-1} \nabla_{\xi\xi} V(\xi)\xi, \tag{20}$$

where $\nabla_{\xi\xi} V(\xi)$ means the Hessian of $V(\xi)$.

Both sides of (20) are left-multiplied by ξ^T,

$$\xi^T \nabla_\xi V(\xi) = \frac{1}{g-1} \xi^T \nabla_{\xi\xi} V(\xi)\xi. \tag{21}$$

With (11), (21) is

$$V(\xi) = \xi^T T(\xi)\xi = \frac{1}{g(g-1)} \xi^T \nabla_{\xi\xi} V(\xi)\xi. \tag{22}$$

The derivative of $V(\xi)$ is

$$\begin{aligned}\dot{V}(\xi) &= \frac{dV(\xi)}{dt}\\ &= \frac{\partial V(\xi)}{\partial x_1}\frac{dx_1}{dt} + \frac{\partial V(\xi)}{\partial x_2}\frac{dx_2}{dt} + \cdots + \frac{\partial V(\xi)}{\partial x_n}\frac{dx_n}{dt} + \frac{\partial V(\xi)}{\partial \sigma(t)}\frac{d\sigma(t)}{dt}\\ &= \dot{\xi}^T \nabla_{\xi} V(\xi).\end{aligned} \tag{23}$$

With (20), (23) is

$$\dot{V}(\xi) = \frac{1}{g-1}\dot{\xi}^T \nabla_{\xi\xi} V(\xi)\xi. \tag{24}$$

With (22), (24) is

$$\begin{aligned}\dot{V}(\xi) &= g\dot{\xi}^T T(\xi)\xi\\ &= g\begin{bmatrix}\dot{x}\\ \dot{\sigma}(t)\end{bmatrix}^T \begin{bmatrix}T_{11}(x,\sigma(t)) & T_{12}(x,\sigma(t))\\ T_{12}^T(x,\sigma(t)) & T_{22}(x,\sigma(t))\end{bmatrix}\begin{bmatrix}x\\ \sigma(t)\end{bmatrix}\\ &= g(\hat{A}(x,\sigma(t))x + B_1 w)^T P(x,\sigma(t))x.\end{aligned} \tag{25}$$

When $w = 0$, (25) is

$$\dot{V}(\xi) = \frac{g}{2}x^T he(\hat{A}^T(x,\sigma(t))P(x,\sigma(t)))x. \tag{26}$$

According to the negative definiteness of the matrix, (14) holds means Θ of (16) is

$$\frac{g}{2}he(\hat{A}^T(x,\sigma(t))P(x,\sigma(t))) + \alpha P(x,\sigma(t)) < 0. \tag{27}$$

(27) is multiplied by the left with x^T and on the right with x,

$$\frac{g}{2}x^T he(\hat{A}^T(x,\sigma(t))P(x,\sigma(t)))x < -\alpha x^T P(x,\sigma(t))x. \tag{28}$$

with (26), (28) is

$$\dot{V}(\xi) < -\alpha V(\xi) < 0, \tag{29}$$

(29) is deduced as

$$V(\xi(t)) < e^{-\alpha(t-t_0)}V(\xi(t_0)). \tag{30}$$

With (30), (19) is

$$\begin{aligned}\|x(t)\| &\le \sqrt{\frac{1}{\varepsilon_1}V(\xi(t))} < \sqrt{\frac{1}{\varepsilon_1}V(\xi(t_0))\cdot e^{-\alpha(t-t_0)}}\\ &\le \sqrt{\frac{\varepsilon_2}{\varepsilon_1}\left\|x(t_0)\right\|^2 \cdot e^{-\alpha(t-t_0)}}\\ &= \sqrt{\frac{\varepsilon_2}{\varepsilon_1}}\left\|x(t_0)\right\| \cdot e^{-\frac{1}{2}\alpha(t-t_0)}, \forall t \ge t_0 \ge 0,\end{aligned} \tag{31}$$

which is simplified as

$$\|x(t)\| < \sqrt{\frac{\varepsilon_2}{\varepsilon_1}}\left\|x(t_0)\right\| \cdot e^{-\frac{1}{2}\alpha(t-t_0)}, \forall t \ge t_0 \ge 0. \tag{32}$$

When $b = \sqrt{\frac{\varepsilon_2}{\varepsilon_1}}$ and $\kappa = \frac{1}{2}\alpha$, (32) is equal to (7), which means that the NPV system (5) is globally exponentially stable with the conditions of (12) and (13).

The robust H_∞ performance of the closed-loop system is proved as following.

(14) holds means Π of (15) is

$$\begin{bmatrix}\Theta & \frac{g}{2}P(x,\sigma(t))B_1 & \hat{C}^T\\ * & -\gamma^2 I & {D_1}^T\\ * & * & -I\end{bmatrix} < 0. \tag{33}$$

Via Schur complementary lemma,[24] (33) is equivalent to

$$\begin{bmatrix} \hat{C}^T \\ {D_1}^T \end{bmatrix} \begin{bmatrix} \hat{C} & D_1 \end{bmatrix} + \begin{bmatrix} \Theta & \frac{g}{2} P(x,\sigma(t)) B_1 \\ * & -\gamma^2 I \end{bmatrix} < 0. \tag{34}$$

(34) is multiplied by the left term $\begin{bmatrix} x^T & w^T \end{bmatrix}$ and the right term $\begin{bmatrix} x^T & w^T \end{bmatrix}^T$,

$$\begin{bmatrix} x \\ w \end{bmatrix}^T \begin{bmatrix} \Theta + \hat{C}^T \hat{C} & \frac{g}{2} P(x,\sigma(t)) B_1 + \hat{C}^T D_1 \\ * & -\gamma^2 I + {D_1}^T D_1 \end{bmatrix} \begin{bmatrix} x \\ w \end{bmatrix} < 0, \tag{35}$$

(35) is expanded as

$$\dot{V}(\xi) + z^T z - \gamma^2 w^T w + \alpha V(\xi) < 0. \tag{36}$$

Since $\alpha V(\xi) > 0$, the term of (36) is

$$\dot{V}(\xi) + z^T z - \gamma^2 w^T w < 0. \tag{37}$$

From (37), the relation is

$$\begin{aligned} J &= \int_0^\infty (z^T z - \gamma^2 w^T w) dt \\ &= \int_0^\infty (\dot{V}(\xi) + z^T z - \gamma^2 w^T w) dt - V(\xi) \\ &< 0, w \in L_2 (0, \infty]. \end{aligned} \tag{38}$$

(38) is equal to (8), which means that the NPV closed-loop system (5) has robust H_∞ performance with Theorem 1. This completes the proof. □

However, (14) contains a coupling term X of (17), which is difficultly solved by the existing methods. Moreover, the closed-loop system matrix $\hat{A}(x, \sigma(t))$ and the EHPLF matrix $P(x, \sigma(t))$ of (17) contain both system states and varying parameter, which cannot be solved by LMI solver. Therefore, it is crucial technology to decouple the nonlinear coupling term X of (17) to transform the EHPLF stability conditions into SOS stability conditions.

3.3 | EHPLF-SOS stability conditions

Definition 1 (SOS[12]). With real polynomials $q_1(x), q_2(x), \dots, q_k(x)$, a real multivariate polynomial $p\left(x_1, x_2, \dots, x_n\right) \triangleq p\,(x)$ is given as

$$p(x) = \sum_{i=1}^{k} q_i^2(x), k \in \mathbf{N}, \tag{39}$$

then $p(x)$ is SOS polynomial, namely $p(x) \in \Sigma_{\mathrm{SOS}}$, Σ_{SOS} is a set of all SOS polynomials.

SOS polynomial is used to transform non-negative polynomial problems into convex optimization problems for solutions by convex optimization algorithms. Here, the stability conditions in Theorem 1 is modified into SOS polynomial to solve NPV controller and to achieve global exponential stability with a robust H_∞ performance for the closed-loop system (5).

Theorem 2. NPV closed-loop system (5) is globally exponentially stable with a robust H_∞ performance under the EHPLF-SOS stability conditions as

$$\begin{aligned} \eta_1^T (P(x,\sigma(t)) - \varepsilon_1 I) \eta_1 &\in \Sigma_{\mathrm{SOS}}, \\ \eta_2^T (\varepsilon_2 I - P(x,\sigma(t))) \eta_2 &\in \Sigma_{\mathrm{SOS}}, \\ -\eta_3^T \left(\Psi + \varepsilon_3 I\right) \eta_3 &\in \Sigma_{\mathrm{SOS}}, \end{aligned} \tag{40}$$

where

$$\Psi = \begin{bmatrix} \Psi_{11} & \Psi_{12} & -G^T C^T - Z^T(x,\sigma(t)) {D_2}^T & -B_1 H(x,\sigma(t)) \\ * & \lambda(G+G^T) & -\lambda(G^T C^T + Z^T(x,\sigma(t)) {D_2}^T) & 0 \\ * & * & -\gamma^2 I & -D_1 H(x,\sigma(t)) \\ * & * & * & I + H(x,\sigma(t)) + H^T(x,\sigma(t)) \end{bmatrix}, \tag{41}$$

where $\Psi_{11} = -he(A(x,\sigma(t))G + B_2 Z(x,\sigma(t))) + \alpha P(x,\sigma(t))$, $\Psi_{12} = \frac{g}{2} P(x,\sigma(t)) + G^T - \lambda(A(x,\sigma(t))G + B_2 Z(x,\sigma(t)))$. G is a constant matrix, $Z(x,\sigma(t))$ is a polynomial matrix, $H(x,\sigma(t))$ is a polynomial matrix, $\lambda > 0$ is a tuning scalar.

Proof. From (40), it is possible to obtain $\Psi < 0$ in (41).

A novel matrix is defined as

$$\Xi^T = \begin{bmatrix} I & \hat{A}(x,\sigma(t)) & 0 & B_1 \\ 0 & \hat{C} & I & D_1 \end{bmatrix}, \tag{42}$$

where

$$\begin{aligned} \hat{A}(x,\sigma(t)) &= A(x,\sigma(t)) + B_2 Z(x,\sigma(t)) G^{-1}, \\ \hat{C} &= C + D_2 Z(x,\sigma(t)) G^{-1}. \end{aligned} \tag{43}$$

With (42), Ψ is multiplied by the left term Ξ^T and the right term Ξ,

$$\begin{bmatrix} \Theta + B_1 {B_1}^T & \frac{g}{2} P(x,\sigma(t)) \hat{C}^T + B_1 {D_1}^T \\ * & -\gamma^2 I + D_1 {D_1}^T \end{bmatrix} < 0. \tag{44}$$

Via Schur complementary lemma,[24] (44) is equivalent to

$$\begin{bmatrix} \Theta & \frac{g}{2} P(x,\sigma(t)) \hat{C}^T & B_1 \\ * & -\gamma^2 I & D_1 \\ * & * & -I \end{bmatrix} < 0. \tag{45}$$

(45) is a dual version of (33) presented in Theorem 1, implying that (40) is a sufficient condition for (7) and (8). Therefore, the NPV closed-loop system (5) is globally exponentially stable with a robust H_∞ performance under the EHPLF-SOS stability conditions in Theorem 2. This completes the proof. □

3.4 | EHPLF-based NPV controller

By comparing (43) with (6), the NPV controller (4) based on EHPLF is

$$u_\tau = K(x,\sigma(t))x = Z(x,\sigma(t)) G^{-1} x, \tag{46}$$

Therefore, if there exists a state feedback controller given by (46) under the EHPLF-SOS stability conditions for the closed-loop system (5), it is referred to as globally exponentially stable and exhibits H_∞ performance.

4 | SIMULATION

A twin-propeller USV is used as the controlled plant. The parameters of NPV model (3) are, $c_1 = -4.0836$, $c_2 = -0.0450$, $c_3 = -2.0114$, $c_4 = 3.2995$. Considering actuator saturation, the controller output moment τ_r is constrained to be in the range of $[-15, 15]\,\mathrm{N \cdot m}$. EHPLF heading control system is shown in Figure 1.

4.1 | Solution of NPV controller based on EHPLF

In EHPLF-SOS stability conditions (40), the H_∞ performance criteria is $\gamma = 1$, the degree of EHPLF is $g = 4$, the tuning scalar is $\lambda = 0.1$, the exponential decay coefficient is $\alpha = 0.1$, and the constants are $\varepsilon_1 = 1 \times 10^{-6}$, $\varepsilon_2 = 5 \times 10^3$, $\varepsilon_3 = 1 \times 10^{-6}$. By using the MATLAB toolbox SOSTOOLS,[25] the EHPLF matrix and controller parameters are obtained,

$$P(x,\sigma(t)) = \begin{bmatrix} P_{11} & P_{12} \\ P_{21} & P_{22} \end{bmatrix}, \tag{47}$$

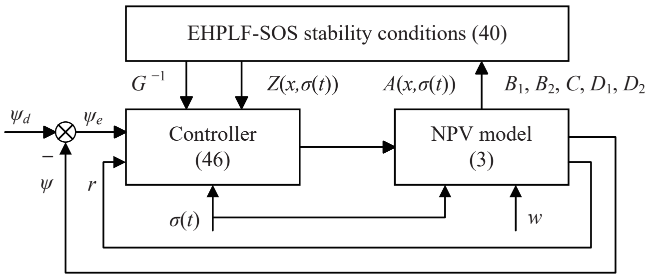

Figure 1 EHPLF heading control system

where

$$
\begin{aligned}
P_{11} &= -0.0054635\sigma(t)^2 + 1.4552\times 10^{-11}\sigma(t)x_1 - 3.638\times 10^{-12}\sigma(t)x_2 \\
&\quad - 0.0054048{x_1}^2 + 3.2742\times 10^{-11}x_1x_2 - 0.005755{x_2}^2, \\
P_{12} &= P_{21} = -2.0903\times 10^{-5}\sigma(t)^2 + 1.819\times 10^{-11}\sigma(t)x_1 + 7.276\times 10^{-12}\sigma(t)x_2 \\
&\quad + 2.3842\times 10^{-5}{x_1}^2 + 2.1828\times 10^{-11}x_1x_2 - 1.4552\times 10^{-11}{x_2}^2, \\
P_{22} &= -0.0066888\sigma(t)^2 + 2.1828\times 10^{-11}\sigma(t)x_1 - 5.8208\times 10^{-11}\sigma(t)x_2 \\
&\quad - 0.0066866{x_1}^2 - 3.638\times 10^{-11}x_1x_2 - 0.0066865{x_2}^2.
\end{aligned}
$$

$$
Z(x,\sigma(t)) = \begin{bmatrix} Z_{11} & Z_{12} \end{bmatrix}, \tag{48}
$$

where

$$
\begin{aligned}
Z_{11} &= -2320.4497\sigma(t)^2 - 8.4765\times 10^{-10}\sigma(t)x_1 - 8.331\times 10^{-10}\sigma(t)x_2 + 1595.82{x_1}^2 + 1.0295\times 10^{-9}x_1x_2 \\
&\quad + 2.4645{x_2}^2 + 3153.7972\sigma(t) + 3.6282\times 10^{-8}x_1 + 8.0734\times 10^{-8}x_2 + 3547.3409, \\
Z_{12} &= -232.1399\sigma(t)^2 - 3.2742\times 10^{-11}\sigma(t)x_1 - 3.638\times 10^{-12}\sigma(t)x_2 + 159.2279{x_1}^2 - 4.0018\times 10^{-11}x_1x_2 \\
&\quad - 3.638\times 10^{-12}{x_2}^2 + 315.2127\sigma(t) + 3.6889\times 10^{-9}x_1 + 8.1091\times 10^{-9}x_2 + 354.2202.
\end{aligned}
$$

$$
G = \begin{bmatrix} -1169.4976 & -116.8834 \\ -108.6262 & -10.8626 \end{bmatrix}. \tag{49}
$$

With (48) and (49), the EHPLF-based NPV controller (46) is

$$
\begin{aligned}
u_\tau &= Z(x,\sigma(t))G^{-1}x \\
&= -1.4149\sigma(t)^2x_1 + 36.5952\sigma(t)^2x_2 + 7.8032\times 10^{-10}\sigma(t){x_1}^2 - 7.1983\times 10^{-9}\sigma(t)x_1x_2 - 1.2858\times 10^{-8}\sigma(t){x_2}^2 \\
&\quad - 5.3185{x_1}^3 + 42.5695{x_1}^2x_2 - 3.6966x_1{x_2}^2 + 39.776{x_2}^3 - 2.5187\sigma(t)x_1 - 1.9169\sigma(t)x_2 + 9.1113\times 10^{-10}{x_1}^2 \\
&\quad - 9.609\times 10^{-9}x_1x_2 - 6.497\times 10^{-9}{x_2}^2 - 7.7227x_1 + 50.4887x_2.
\end{aligned} \tag{50}
$$

4.2 | Nonlinear heading performance analysis

The nonlinearity of NPV model (3) is caused by the high-order term of yaw velocity. Different yaw velocities reflect the varying degree of nonlinearity for NPV system. To compare the nonlinear control performance of EHPLF and PLF[10] methods on the NPV system, external disturbance is $w = 0$, the surge velocity is $u = 1.5$ m/s, and the desired heading angle is $\psi_d = \pi/3 + 0.4\sin(0.05\beta_1\pi t)$ rad[26], yaw velocity is $r = \dot{\psi}_d = 0.02\beta_1\pi\cos(0.05\beta_1\pi t)$ rad/s. Different values of $\beta_1 (\beta_1 = 1, 2, 4)$ indicate different levels of nonlinearity. Figure 2 shows the heading angle responses of the system for $\beta_1 = 2$ and 4. Figure 3 shows the heading angle errors ψ_e for different values of β_1.

Figure 2A shows the transient time of EHPLF is 0.580 s and PLF is 1.180 s when $\beta_1 = 2$. Figure 2B shows the transient time for these two methods are 0.624 s and 1.420 s when $\beta_1 = 4$, respectively. The transient time of the EHPLF control system is about half of PLF control system. Figure 3 shows the steady-state errors of the heading angle with EHPLF method is ±0.008012 rad of $\beta_1 = 1$, ±0.01602 rad of $\beta_1 = 2$, and ±0.03203 rad of $\beta_1 = 4$, respectively, while it is ±0.01915 rad of $\beta_1 = 1$, ±0.03818 rad of $\beta_1 = 2$, and ±0.07544 rad of $\beta_1 = 4$ for the PLF method respectively. Moreover, the steady-state errors increase as

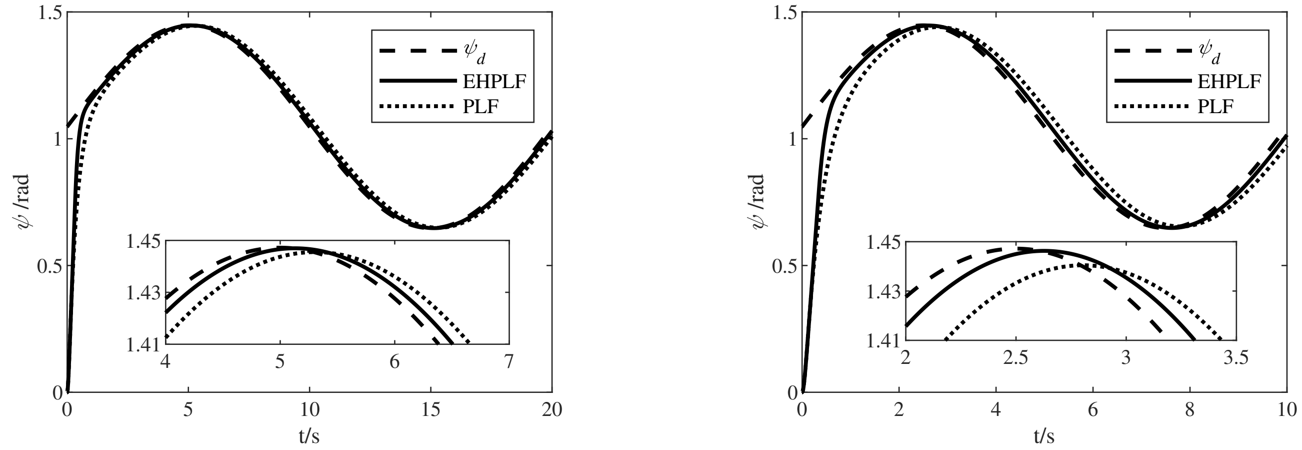

(A) **(B)**

Figure 2 Heading angle responses. (A) $\beta_1 = 2$; (B) $\beta_1 = 4$

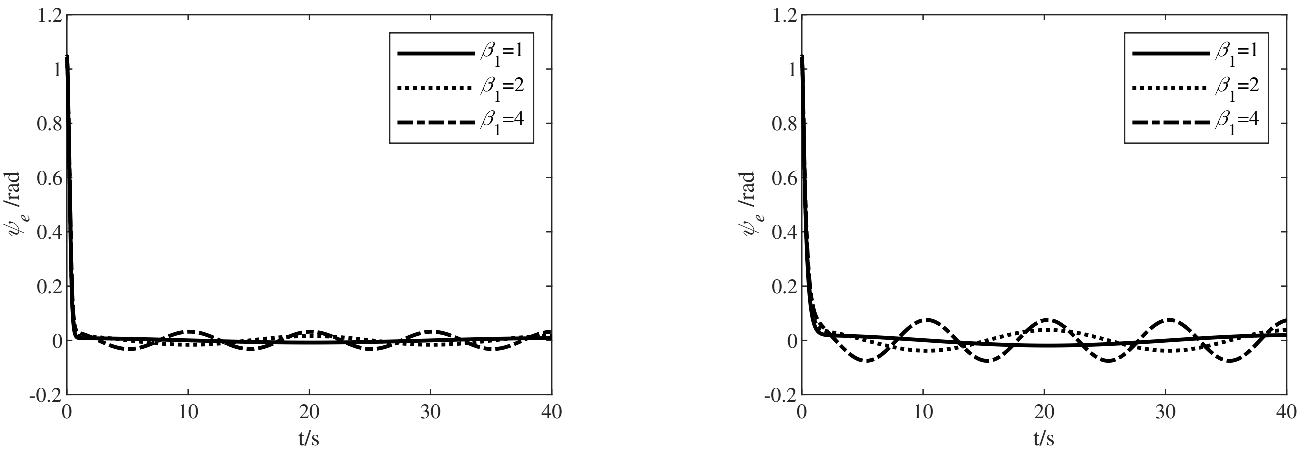

(A) **(B)**

Figure 3 Heading angle errors. (A) EHPLF method; (B) PLF method

β_1 increases, but the errors by EHPLF method always is exhibits smaller than PLF. Therefore, EHPLF can better suppress the nonlinear characters of NPV system compared with PLF.

4.3 | Analysis of heading performance with varying surge velocity

To analyze the suppression of varying parameter of surge velocity, the external disturbance is $w = 0$, the desired heading angle is $\psi_d = \pi/3$ rad, and the varying surge velocity is $u = (\sin(\beta_2 t) + 1)$ m/s.[13] $\beta_2(\beta_2 = 0.1, 1, 2, 3)$ represents different rates of varying parameters. Figure 4 shows the responses of the heading control system when $\beta_2 = 2$. Figure 5 shows the variation of yaw velocity r for different values of β_2 by the two methods.

Figure 4A shows the transient time of EHPLF and PLF control systems is 0.525 s and 0.912 s when $\beta_2 = 2$, which implies the EHPLF control system still exhibits a shorter transient time. Figure 4B shows the yaw velocity variation by EHPLF is smoother

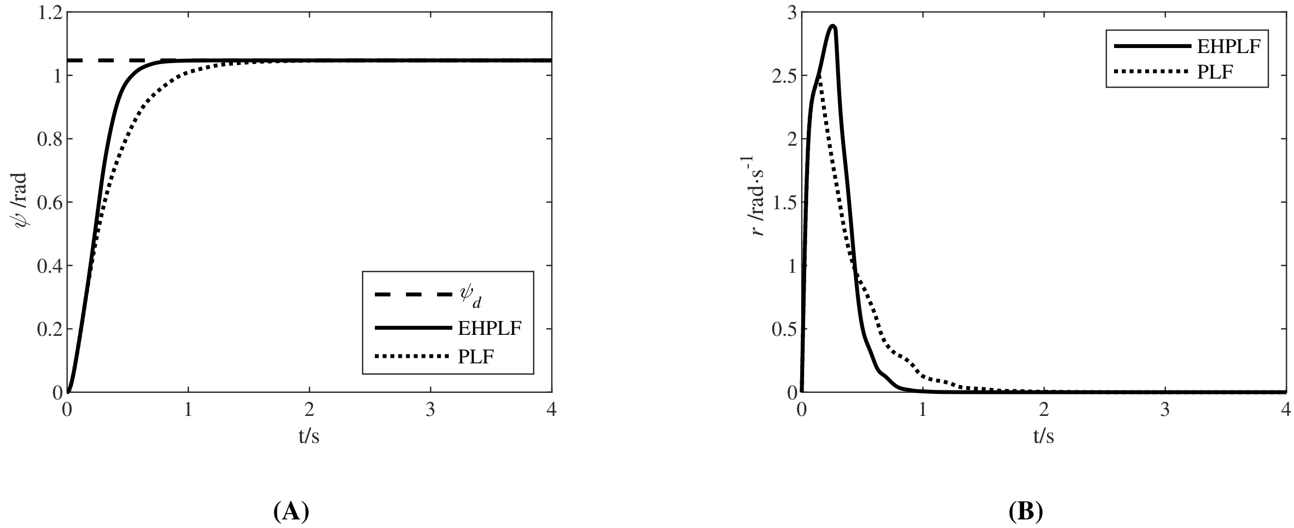

Figure 4 The responses of heading control system. (A) heading angle responses; (B) yaw velocity responses

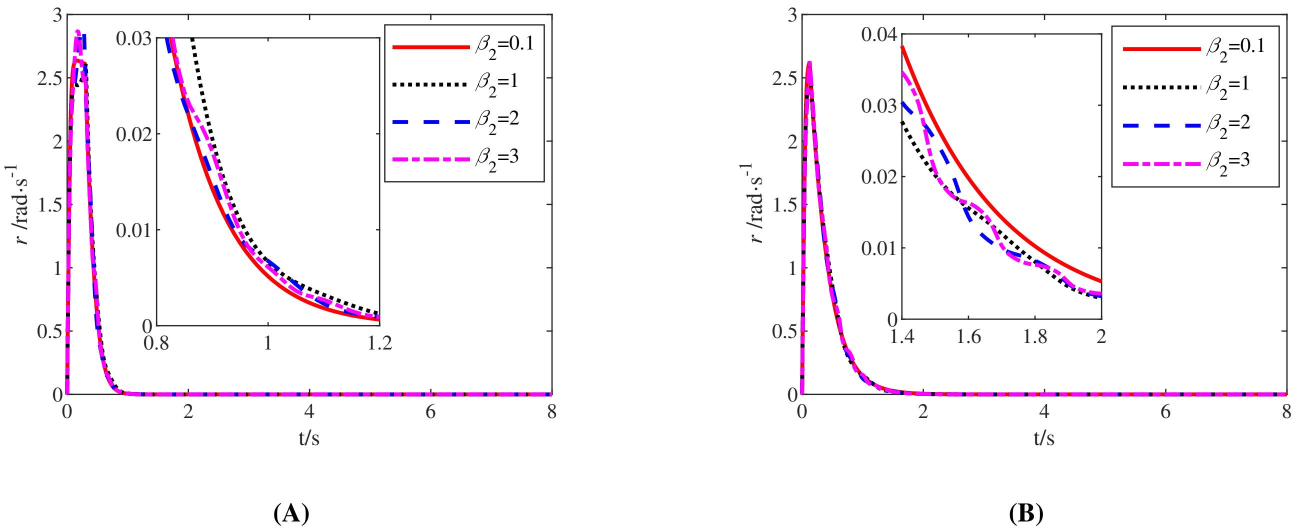

Figure 5 Yaw velocity responses. (A) EHPLF method; (B) PLF method

than that by PLF, which enhances the stable navigation of USV. Figure 5 shows that the fluctuations of the state r increase as β_2 increases of both EHPLF system and PLF system. As it can be seen that the fluctuations of the state r of EHPLF system are smaller than those of PLF system. Therefore, the EHPLF method can effectively suppress the adverse effects of varying surge velocity u on NPV system, and exhibits a faster response and stronger robustness.

4.4 | Analysis of heading performance with external disturbance

In order to suppress unknown wave disturbances, external wave disturbances are introduced as[27]

$$w = A_w \sin(\omega_e t + \vartheta), \tag{51}$$

where $A_w = 0.3$ is the wave amplitude, $\vartheta = 0$ rad is the random phase, ω_e is the encounter frequency which is assumed to be distributed randomly within the range [0.3, 1.3] rad/s. The desired heading angle is $\psi_d = \pi/3$ rad, the varying surge velocity is $u = (\sin(t) + 1)$ m/s. Figure 6 shows the responses of heading angle by the two methods.

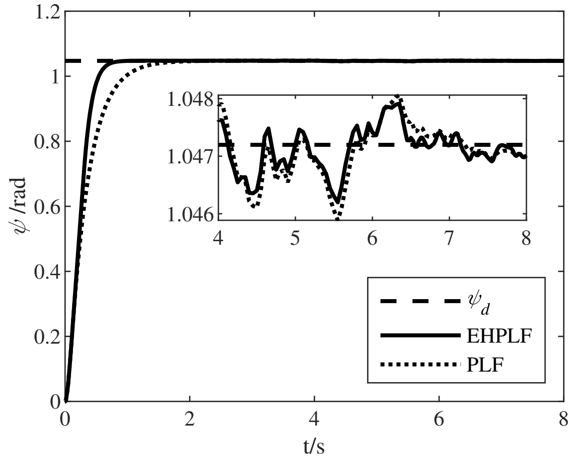

Figure 6 The responses of heading angle

In Figure 6, EHPLF system exhibits the transient time and the steady-state error of 0.555 s and ±0.00105 rad respectively, while PLF system shows the transient time and the steady-state error of 0.921 s and ±0.00131 rad. Compared to the PLF system, EHPLF system has the shorter transient time, the smaller steady-state error, and the stronger robustness to suppress external disturbances.

5 | CONCLUSIONS

A robust H_∞ heading control method is proposed by EHPLF for NPV model of the USV, which effectively enhances the system performance. Firstly, a NPV model of heading error is established with the nonlinearity of the yaw velocity and the varying surge velocity, and a general form of state feedback controller is constructed by the exponential stability conditions with a robust H_∞ performance. Secondly, a Lyapunov matrix is defined with full states and varying parameter with the idea of HPLF. By utilizing the Euler's homogeneity relation, the robust H_∞ global exponential stability conditions are deduced for NPV system, namely EHPLF stability conditions. Thirdly, since EHPLF stability conditions consist of a set of nonlinear coupled inequalities, they cannot be directly solved by SOSTOOLS. The EHPLF stability conditions are decoupled by the matrix transformation to obtain the EHPLF-SOS stability conditions, which are solved directly to obtain the parameters of the NPV controller. Finally, NPV controller based on EHPLF is applied to simulate the USV heading control. The simulation results indicate that,

1. Both the transient time and steady-state errors of the EHPLF system are approximately 50% of those of the PLF system for different degrees of nonlinear.
2. The EHPLF system also exhibits a transient time of about 50% of the PLF system, and has the smaller fluctuations of the state r than those of PLF system with the different varying parameter of the surge velocity.
3. With unknown wave disturbances, the EHPLF system also exhibits smaller steady-state errors than those of the PLF system.

ACKNOWLEDGMENTS

This work was supported by the Science and Technology Guidance Project of Fujian (2019H0007) and the National Natural Science Foundation of China (51977040).

References

1. Abrougui H, Nejim S, Hachicha S, Zaoui C, Dallagi H. Modeling, parameter identification, guidance and control of an unmanned surface vehicle with experimental results. *Ocean Engineering* 2021; 241: 110038. doi: 10.1016/j.oceaneng.2021.110038

2. Hu C, Wang R, Yan F, Chen N. Robust composite nonlinear feedback path-following control for underactuated surface vessels with desired-heading amendment. *IEEE Transactions on Industrial Electronics* 2016; 63(10): 6386–6394. doi: 10.1109/TIE.2016.2573240

3. Wang YL, Han QL. Network-based heading control and rudder oscillation reduction for unmanned surface vehicles. *IEEE Transactions on Control Systems Technology* 2016; 25(5): 1609–1620. doi: 10.1109/TCST.2016.2617321

4. Chu R, Liu Z, Chu Z. Improved super-twisting sliding mode control for ship heading with sideslip angle compensation. *Ocean Engineering* 2022; 260: 111996. doi: 10.1016/j.oceaneng.2022.111996

5. Juang JY, Chang B. Robust control theory applied to ship maneuvering. In: IEEE. Proceedings of the 38th IEEE Conference on Decision and Control (Cat. No.99CH36304); 1999; Phoenix, USA: 2186–2191

6. Huang Y, Huang P. An improved bounded real lemma for H_∞ robust heading control of unmanned surface vehicle. *Proceedings of the Institution of Mechanical Engineers, Part I: Journal of Systems and Control Engineering* 2023. doi: 10.1177/09596518231172264

7. Xiong J, He Y, Han J, Yuan M. Robust heading control of an unmanned surface vehicle based on LPV model. *Journal of System Simulation* 2020; 32(8): 1598–1605. doi: 10.16182/j.issn1004731x.joss.18-0043

8. Huang Y, Liu Z, Huang W, Chen S. Robust H_∞ control for nonlinear course system of unmanned surface vessel with polytopic uncertainty based on sum of squares. *Transactions of the Institute of Measurement and Control* 2021; 43(2): 390–399. doi: 10.1177/0142331220957750

9. Huang Y, Lin T, Huang W. Extended bounded real lemma based sum of squares for static output feedback H_∞ heading control. *International Journal of Robust and Nonlinear Control* 2022; 32(14): 7879–7895. doi: 10.1002/rnc.6249

10. Fu R, Zeng J, Duan Z. H_∞ mixed stabilization of nonlinear parameter-varying systems. *International Journal of Robust and Nonlinear Control* 2018; 28(17): 5232–5246. doi: 10.1002/rnc.4304

11. Fu R, Sun H, Zeng J. Exponential stabilisation of nonlinear parameter-varying systems with applications to conversion flight control of a tilt rotor aircraft. *International Journal of Control* 2019; 92(11): 2473–2483. doi: 10.1080/00207179.2018.1442022

12. Lu L, Fu R, Zeng J, Duan Z. On the domain of attraction and local stabilization of nonlinear parameter-varying systems. *International Journal of Robust and Nonlinear Control* 2020; 30(1): 17–32. doi: 10.1002/rnc.4746

13. Huang Y, Huang P. H_∞ Robust Heading Control for Nonlinear Parameter-Varying Unmanned Surface Vehicle. *Control and Decision* 2023. doi: 10.13195/j.kzyjc.2022.2028

14. Chesi G, Garulli A, Tesi A, Vicino A. Homogeneous Lyapunov functions for systems with structured uncertainties. *Automatica* 2003; 39(6): 1027–1035. doi: 10.1016/S0005-1098(03)00039-6

15. Tanaka K, Yoshida H, Ohtake H, Wang HO. A sum-of-squares approach to modeling and control of nonlinear dynamical systems with polynomial fuzzy systems. *IEEE Transactions on Fuzzy systems* 2008; 17(4): 911–922. doi: 10.1109/TFUZZ.2008.924341

16. Bernal M, Sala A, Jaadari A, Guerra TM. Stability analysis of polynomial fuzzy models via polynomial fuzzy Lyapunov functions. *Fuzzy Sets and Systems* 2011; 185(1): 5–14. doi: 10.1016/j.fss.2011.07.008

17. Zhao Y, He Y, Feng Z, Shi P, Du X. Relaxed sum-of-squares based stabilization conditions for polynomial fuzzy-model-based control systems. *IEEE Transactions on Fuzzy Systems* 2018; 27(9): 1767–1778. doi: 10.1109/TFUZZ.2018.2889019

18. Khooban MH, Vafamand N, Dragičević T, Blaabjerg F. Polynomial fuzzy model-based approach for underactuated surface vessels. *IET Control Theory & Applications* 2018; 12(7): 914–921. doi: 10.1049/iet-cta.2017.1106

19. Lo JC, Lin C. Polynomial fuzzy observed-state feedback stabilization via homogeneous Lyapunov methods. *IEEE Transactions on Fuzzy Systems* 2017; 26(5): 2873–2885. doi: 10.1109/TFUZZ.2017.2786211

20. Lo JC, Liu JW. Polynomial static output feedback H_∞ control via homogeneous Lyapunov functions. *International Journal of Robust and Nonlinear Control* 2019; 29(6): 1639–1659. doi: 10.1002/rnc.4451

21. Sabbaghian-Bidgoli F, Farrokhi M. Robust fuzzy observer-based fault-tolerant control: A homogeneous polynomial Lyapunov function approach. *IET Control Theory & Applications* 2023; 17(1): 74–91. doi: 10.1049/cth2.12362

22. Skulstad R, Li G, Fossen TI, Vik B, Zhang H. A hybrid approach to motion prediction for ship docking—Integration of a neural network model into the ship dynamic model. *IEEE Transactions on Instrumentation and Measurement* 2020; 70: 1–11. doi: 10.1109/TIM.2020.3018568

23. Li X, Song S, Wu J. Exponential stability of nonlinear systems with delayed impulses and applications. *IEEE Transactions on Automatic Control* 2019; 64(10): 4024–4034. doi: 10.1109/TAC.2019.2905271

24. Ito H, Krstić M. Recursive scaling design for robust global nonlinear stabilization via output feedback. *International Journal of Robust and Nonlinear Control* 2000; 10(10): 821–848. doi: 10.1002/1099-1239(200008)10:10<821::AID-RNC526>3.0.CO;2-M

25. Prajna S, Papachristodoulou A, Parrilo PA. Introducing SOSTOOLS: A general purpose sum of squares programming solver. In: Proceedings of the 41st IEEE Conference on Decision and Control; 2002; Las Vegas, USA: 741–746

26. Gonzalez-Garcia A, Castañeda H. Guidance and control based on adaptive sliding mode strategy for a USV subject to uncertainties. *IEEE Journal of Oceanic Engineering* 2021; 46(4): 1144–1154. doi: 10.1109/JOE.2021.3059210

27. Luo W, Zhang F. Time-invariant Discontinuous Feedback Stablization of Underactuated Surface Vessel under Wave Disturbance. In: IEEE. 2021 International Conference on Security, Pattern Analysis, and Cybernetics (SPAC); 2021; Chengdu, China: 466–469